A Highly Effective Impulse Noise Detection Algorithm for Switching Median Filters

Fei Duan and Yu-Jin Zhang, *Senior Member, IEEE*

***Abstract*—Under the framework of switching median filtering, a highly effective algorithm for impulse noise detection is proposed aiming at providing solid basis for subsequent filtering. This algorithm consists of two iterations to make the decision as accurate as possible. Two robust and reliable decision criteria are proposed for each iteration. Extensive simulation results show that the false alarm rate and miss detection rate of the proposed algorithm are both very low and substantially outperform existing state-of-the-art algorithms. At the same time, the proposed algorithm is in principle simpler as it is intuitive and it is easy to implement as it has uncomplicated structure and few codes.**

***Index Terms*—Impulse noise, noise detection, salt-and-pepper noise, switching median filter.**

I. Introduction

In the process of image acquisition and transmission, impulse noises often cause serious degradation of the image quality. Various filtering algorithms [1]–[11] have been proposed. Among them, the family of median filters is the most popular and holds a dominant position in this area for its outstanding noise suppression ability. The most representative paradigm in this family is known as "Switching Median Filtering" (SMF) [3], which partitions the whole filtering process into two sequential steps—noise detection and filtering. By utilizing the *a priori* knowledge obtained from the noise detection step, the filtering step could be more targeted and does not need to touch those uncorrupted pixels. Obviously the accuracy of the noise detection is critical to the final result.

Since this letter mainly focuses on the impulse noise detection approaches under SMF, the following literature review only pays close attentions to the detection strategies of three representative algorithms among the state-of-art progresses [5]–[11]. In [5], an impulse noise identification algorithm is proposed based on the minimum absolute values of four convolutions deduced from the 1-D Laplacian operator. Since this set of convolutionary values jointly encode the intensity difference between each pixel and its neighbors essentially, these useful latent information are not thoroughly exploited in this way. Thus the performance degradation of this detector is very significant with the growth of the noise density. The boundary discriminative noise detection (BDND) algorithm [6] is probably the one who makes the most progress under the SMF framework in recent years. It uses the local histogram to adaptively determine the decision boundaries between noise-free and corrupted pixels. A pixel is first examined from its 21×21 neighborhood. If it is classified into the "corrupted" category, then a validation stage is conducted by narrowing its neighborhood to 3×3. Obviously, this algorithm hopes to examine the current pixel from coarse to fine. But in the refining stage, it is unlikely that the decision boundaries deduced from the local histogram of only 9 pixels are very reliable. In [11], the proposed switching-based adaptive weighted mean (SAWM) algorithm adopts the strategy of comparing the minimum absolute value of four mean differences between the current pixel and its neighbors with a predefined threshold to determine whether current pixel is corrupted.

In this letter, we propose a new and improved impulse noise detection algorithm based on the BDND detector. Like BDND, the proposed algorithm also adopts the coarse-to-fine strategy. In the first stage, we redefine the decision rule by utilizing the characteristics of the impulse noise model. And in the second stage, we propose a validation criterion based on a group of newly designed convolutionary kernels. Extensive simulation results show that the proposed detector's false alarm rate and miss detection rate are both amazingly low even when noise density is up to 90% and substantially outperforms existing state-of-the-art algorithms. At the same time, the proposed algorithm is in principle simpler as it is intuitive and it is easy to implement as it has uncomplicated structure and few codes.

The rest of the letter is organized as follows. Section II provides an overview of the BDND detector and describes its merits and limitations. In Section III, the motivation and basic principles of our proposed method are presented in detail. Section IV describes the simulation results and provides an analytical discussion on the performance of our algorithm. Finally, Section V gives our conclusions in summarizing the work and improvements done on the BDND framework.

II. The BDND Detector

The basic strategy of BDND is to examine each pixel in its neighborhood from coarse to fine. If current pixel is categorized into "corrupted" in both "coarse" and "fine" stages, then it is considered to be contaminated. So the most critical part of this paradigm is the determination of the decision boundaries. This criterion can be summarized as follows:

$$class(x_{i,j}) = \begin{cases} \text{Pepper Noise}, & x_{i,j} \le b_1 \\ \text{Uncorrupted}, & b_1 < x_{i,j} \le b_2 \\ \text{Salt Noise}, & x_{i,j} > b_2 \end{cases} \quad (1)$$

Manuscript received January 14, 2010; revised April 09, 2010; accepted April 16, 2010. Date of publication May 18, 2010; date of current version May 26, 2010. This work was supported in part by the National Natural Science Foundation of China under Grant 60872084. The associate editor coordinating the review of this manuscript and approving it for publication was Prof. Dimitrios Androutsos.

The authors are with the Department of Electronic Engineering, Tsinghua University, Beijing 100084, China (e-mail: duanf03@mails.thu.edu.cn; zhangyj@tsinghua.edu.cn).

Color versions of one or more of the figures in this paper are available online at http://ieeexplore.ieee.org.

Digital Object Identifier 10.1109/LSP.2010.2049515

where $x_{i,j}$ is the intensity of the pixel being considered, and b_1, b_2 are the two decision boundaries.

The following steps are used by the BDND algorithm.

1) For each pixel x_{ij} in the image, impose a 21×21 window centers on x_{ij}.
2) Sort the pixels lie in the window region to an ordered vector $\mathbf{v}_o$ and find the median med.
3) Compute the difference vector of $\mathbf{v}_o$.
4) Find the pixels which correspond to the maximum differences in the intervals of $[0, med]$ and $(med, 255]$. And set these two pixels' intensities as the decision boundaries b_1 and b_2 respectively.
5) Classify the pixels in current window into three clusters according to (1).
6) Validate the noisy candidates by imposing a 3×3 window, and repeat steps 2)–5).

According to the above steps of the BDND algorithm, we can see that in the first stage when a 21×21 window is imposed on each pixel, more than 400 pixels are taken into account to calculate the local histogram. Obviously, this order of magnitude is statistically meaningful. Hence the reliability of the two decision boundaries is acceptable. And the simulation results in [6] have proved its effectiveness when the imposed window is at this scale. But in the second validation stage of BDND, we see that this algorithm reduces the window's dimension to 3×3. That is, only nine pixels are taken into account to calculate the local histogram. Obviously, this order of magnitude lacks statistical significance seriously. And the effectiveness of the validation is dramatically weakened. To illustrate this point, we give two misclassified cases of BDND as shown in Fig. 1. These examples are sampled from the "Lena" image which is contaminated with 20% salt-and-pepper noise. Only the 7×7 neighborhood of these two pixels are displayed in Fig. 1(b) and Fig. 1(c) for lack of space. The pixels enclosed by circles correspond to false-detected examples and the pixels enclosed by rectangles are the miss-detected examples. According to the criterion of BDND, these pixels are misclassified in both of the two iterations of decision. Whereas in our proposed algorithm, these cases can be avoided.

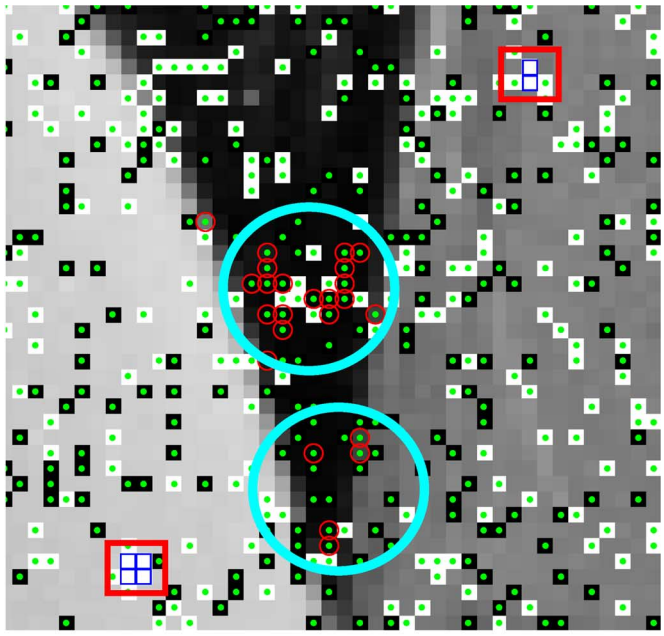

(a)

12	7	9	9	5	255	29
9	7	5	7	4	5	30
4	5	9	8	4	9	39
4	5	5	4	4	0	255
3	255	4	4	4	16	255
11	6	5	255	7	15	255
0	4	8	9	255	78	118

(b)

119	124	119	118	125	255	115
122	116	118	0	0	255	118
121	117	123	255	118	115	115
255	123	255	255	255	120	255
122	120	255	255	119	116	120
116	120	0	119	118	120	119
121	125	125	255	119	122	0

(c)

Fig. 1. Miss detection and false detection examples. (a) A subimage cropped from the Lena image, (b) 7×7 neighborhood of a false detection sample in Fig. 1(a), (c) 7×7 neighborhood of a miss detection sample in Fig. 1(a).

III. The Proposed Algorithm

Although the "salt-and-pepper" noise model is possibly the one who receives the most concerns, it is only a special case of "Noise Model 3" in [6]. So we choose the latter model as the object of study to make our algorithm more realistic and more general. In this model, impulse noises uniformly distribute over two length-m intervals which lie in the two ends of the intensity range. We denote the intensity values of the pixels at location (i, j) in the original and corrupted image as $s_{i,j}$ and $x_{i,j}$ respectively, in which the probability density function of $x_{i,j}$ is

$$f(x_{i,j}) = \begin{cases} \frac{p}{2m}, & 0 \le x_{i,j} < m \\ 1 - \frac{p}{m}, & x_{i,j} = s_{i,j} \\ \frac{p}{2m}, & 255 - m < x_{i,j} \le 255 \end{cases} \tag{2}$$

where p is the noise density.

Like BDND, our proposed algorithm also consists of two iterations and all pixels in the noisy image are examined. Only when a pixel is judged as noise candidate, it will be piped into the second validation stage. And only when a pixel is classified into the "Noise" class in both stages, it will be considered to be a "true" impulse noise pixel. From above analysis we can see that the main weakness of BDND resides in the validation stage. And lack of statistical significance is the root cause of misclassification. To make the decisions in both iterations more robust and reliable, we propose two new strategies of computing the decision boundaries for both iterations separately. First, we redefine the classification criterion as follows in view of the distinctive characteristics of the intensity distribution of the impulse noise we care about.

$$class(x_{i,j}) = \begin{cases} \text{Pepper Noise}, & x_{i,j} \le \min(b_1, m) \\ \text{Salt Noise}, & x_{i,j} \ge \max(b_2, 255 - m) \\ \text{Uncorrupted}, & \text{otherwise.} \end{cases} \tag{3}$$

In (3), the strategy of computing b_1 and b_2 is the same as BDND. By encoding the *a priori* knowledge of the noise characteristics into the classifier, the decision boundaries calculated from the local histogram get the chance to be rectified. And the noise-free pixels whose intensities do not lie in the "noise" intervals will not have the chance of entering the second iteration.

In order to enhance the reliability of the decision boundaries, simply expanding the window size in the second iteration obviously is not a wise choice, for this sort of action would undoubtedly incur significant loss of efficiency. The basic philosophy of our method is to find a way to accurately quantify the intensity differences between the current pixel and its neighbors in four

$$\begin{bmatrix} 0 & 0 & 0 & 0 & 0 & 0 & 0 \\ 0 & 0 & 0 & 0 & 0 & 0 & 0 \\ 0 & 0 & 0 & 0 & 0 & 0 & 0 \\ -1 & -1 & -1 & 6 & -1 & -1 & -1 \\ 0 & 0 & 0 & 0 & 0 & 0 & 0 \\ 0 & 0 & 0 & 0 & 0 & 0 & 0 \\ 0 & 0 & 0 & 0 & 0 & 0 & 0 \end{bmatrix}$$

(a)

$$\begin{bmatrix} 0 & 0 & 0 & -1 & 0 & 0 & 0 \\ 0 & 0 & 0 & -1 & 0 & 0 & 0 \\ 0 & 0 & 0 & -1 & 0 & 0 & 0 \\ 0 & 0 & 0 & 6 & 0 & 0 & 0 \\ 0 & 0 & 0 & -1 & 0 & 0 & 0 \\ 0 & 0 & 0 & -1 & 0 & 0 & 0 \\ 0 & 0 & 0 & -1 & 0 & 0 & 0 \end{bmatrix}$$

(b)

$$\begin{bmatrix} 0 & 0 & 0 & 0 & 0 & 0 & -1 \\ 0 & 0 & 0 & 0 & 0 & -1 & 0 \\ 0 & 0 & 0 & 0 & -1 & 0 & 0 \\ 0 & 0 & 0 & 6 & 0 & 0 & 0 \\ 0 & 0 & -1 & 0 & 0 & 0 & 0 \\ 0 & -1 & 0 & 0 & 0 & 0 & 0 \\ -1 & 0 & 0 & 0 & 0 & 0 & 0 \end{bmatrix}$$

(c)

$$\begin{bmatrix} -1 & 0 & 0 & 0 & 0 & 0 & 0 \\ 0 & -1 & 0 & 0 & 0 & 0 & 0 \\ 0 & 0 & -1 & 0 & 0 & 0 & 0 \\ 0 & 0 & 0 & 6 & 0 & 0 & 0 \\ 0 & 0 & 0 & 0 & -1 & 0 & 0 \\ 0 & 0 & 0 & 0 & 0 & -1 & 0 \\ 0 & 0 & 0 & 0 & 0 & 0 & -1 \end{bmatrix}$$

(d)

Fig. 2. Four directional convolutionary kernels.

representative directions. The idea is inspired by [5], but in considering both accuracy and efficiency, our strategy of using the four descriptors and the size of our kernels are different from [5]. The dimension of the neighborhood of each pixel we adopt is 7×7 and the directions we care about are $0, \pi/4, \pi/2, 3\pi/4$. Thus four kernels can be constructed as shown in Fig. 2.

Then by convolving the group of kernels with the noise image, every pixel get four convolutionary results. We take the absolute values of the convolutionary values as the metrics of the intensity homogeneity of the neighborhood of the current pixel. This computation strategy can be formulated as follows:

$$\mathbf{V}_{ij}^{(k)} = \left| \mathbf{I} \otimes \mathbf{Ker}^{(k)} \right|_{ij}, \quad k = 1, \cdots, 4 \tag{4}$$

where $\mathbf{I}$ is the noisy image, $\mathbf{Ker}^{(k)}$ is the k^{th} kernel we designed, $\mathbf{V}_{ij}^{(k)}$ represents the k^{th} absolute convolutionary value for pixel $\mathbf{I}_{ij}$ and $\otimes$ denotes the convolution operator.

In [5], only the minimum of the four descriptors is used. Since the intensity homogeneity information is jointly encoded in the four descriptors, this strategy does not fully exploit the latent information. And more seriously, this rule only favors the detection of isolated impulse noises by only comparing the minimum with a given threshold to decide whether current pixel is corrupted. If the noise density is high, it is very common that several impulse noises of the same kind ("salt" or "pepper") be adherent in certain direction or form clusters. In these cases, this rule will completely fail. In our algorithm, we utilize both the minimum and maximum of aforementioned four descriptors at the same time. These two values can be calculated according to (5). Our intuition is that only joint utilization of these descriptors can provide reliable decisions.

$$\begin{cases} R_{ij}^{min} = \min\left\{ \mathbf{V}_{ij}^{(1)}, \mathbf{V}_{ij}^{(2)}, \mathbf{V}_{ij}^{(3)}, \mathbf{V}_{ij}^{(4)} \right\} \\ R_{ij}^{max} = \max\left\{ \mathbf{V}_{ij}^{(1)}, \mathbf{V}_{ij}^{(2)}, \mathbf{V}_{ij}^{(3)}, \mathbf{V}_{ij}^{(4)} \right\} \end{cases}. \tag{5}$$

And our classification rule is formulated as follows: if $R_{ij}^{min} > T_1$ or $R_{ij}^{max} - R_{ij}^{min} > T_2$, then pixel I_{ij} is corrupted; otherwise I_{ij} is not corrupted. In this criterion, T_1 and T_2 are two predefined threshold values.

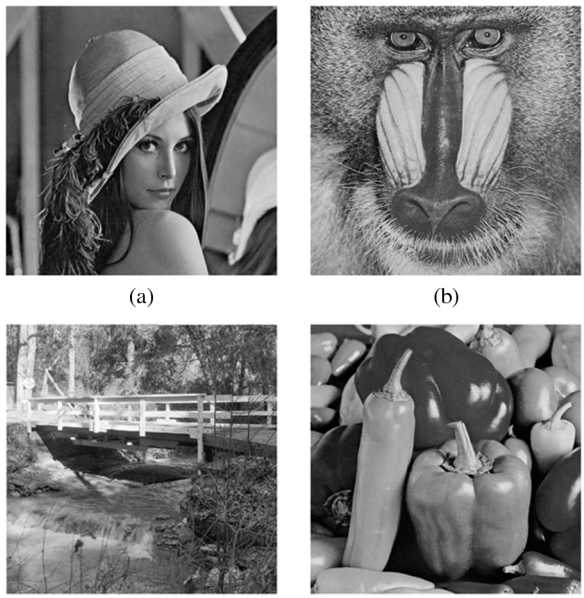

(a) (b) (c) (d)

Fig. 3. Testing images we used. (a) Lena, (b) Baboon, (c) Bridge, (d) Peppers.

We use such a logical rule as the classification criterion due to the following reasons.

1) If the current pixel corresponds to an isolated impulse noise, then each of the four convolutionary values must be quite large.
2) If there are only very few noises in the neighborhood of the current pixel, all the four convolutionary values must be quite small and the differences among these values are less significant.
3) If the current pixel is not corrupted but is classified into the corrupted category, then the difference among the four convolutionary values should be below a certain level since we assume these impulse noises are evenly distributed over the given image.

IV. Experiment Results and Discussions

To demonstrate the effectiveness of our algorithm on detecting impulse noises, we compare our results with two of the most representative state-of-art algorithms—BDND and SAWM [11]. Extensive simulations are carried on four well-known images: Lena, Baboon, Peppers, and Bridge, which are shown in Fig. 3. The bit depth of these images are 8 and the resolution of them are all 512×512.

In order to compare with other two algorithms, we select the "salt-and-pepper" noise model in which gray-level 0 represents "pepper" and 255 represents "salt." These noise are evenly scattered over the whole image. The noise density we considered ranges from 10% to 90% with incremental step 10%.

To make our detection algorithm be able to implement on the whole image region, we extend each of the four boundaries of the testing image through mirror-reflecting by ten pixels. And the two thresholds T_1 and T_2 are respectively set to 5/255 and 1/255 (assuming the intensity of the image has been normalized). The evaluation indices we considered are the number of miss detection that represents the number of noise being misdetected and the number of false alarm that represents the number of noise-free pixels that are misclassified as noise. These two indicators are computed by comparing the output of BDND's and

TABLE I
NUMBERS OF MISS DETECTION AND FALSE ALARM.
(a) LENA, (b) BABOON, (c) BRIDGE, (d) PEPPERS

	Miss Detection (MD)			False Alarm (FA)		
Noise %	BDND	SAWM	OURS	BDND	SAWM	OURS
20	0	0	0	2	0	0
40	0	0	0	5	0	0
60	0	0	0	6	0	0
80	21	0	0	10	0	0
90	190	0	0	5	0	0

(a)

	Miss Detection (MD)			False Alarm (FA)		
Noise %	BDND	SAWM	OURS	BDND	SAWM	OURS
20	0	6	0	30	51	4
40	0	9	0	29	2	3
60	0	8	0	24	1	1
80	6	5	0	21	1	1
90	272	2	0	16	0	1

(b)

	Miss Detection (MD)			False Alarm (FA)		
Noise %	BDND	SAWM	OURS	BDND	SAWM	OURS
20	0	179	0	2433	95	366
40	0	288	0	1805	45	275
60	0	344	0	1419	37	184
80	0	293	0	1092	28	95
90	0	202	0	1244	18	46

(c)

	Miss Detection (MD)			False Alarm (FA)		
Noise %	BDND	SAWM	OURS	BDND	SAWM	OURS
20	0	18	0	370	22	173
40	0	14	0	370	0	126
60	0	21	0	290	0	83
80	12	5	0	127	0	39
90	51	207	0	336	0	18

(d)

SAWM's noise detection modules with the ground-truth binary decision map. To make the detection results more objective and more accurate, we repeat the noise adding and detection procedures 20 times independently for each noise density and take the average as the final results. Due to space limitation, only the results corresponding to noise densities of 20%, 40%, 60%, 80% and 90% are listed.

From Table I we can see that our proposed detection algorithm achieves very amazing *ZERO* miss detection rate while maintaining a rather low false alarm rate. In other words, our method is more powerful to discover impulse noise and corrupted pixels have little chance to be omitted. It is not difficult to infer that in the context of impulse noise suppression false detections are more harmful than miss detections. The reason resides in the fact that if the noise pixels are misdetected, they will lose the chance of being restored. And by adopting proper filtering scheme, those false detected pixels would NOT be significantly affected. From this point of view, our proposed method has great superiority over the state-of-the-art methods and undoubtedly will provide solid basis for subsequent filtering stage.

By analyzing the simulation results, we can also get another important conclusion. We notice that the detection results of "Bridge" and "Pepper" are significantly inferior to another two images. This can be simply explained with the principle of the classical Bayesian decision theory. We know that in the context of two-class classification problem, when the tails of the p.d.f of certain class becomes heavier, the error classification probability will become larger, whereas the tails of the histograms of "Bridge" and "Pepper" happen to be more heavier than other two testing images.

V. CONCLUSION

In this letter, an exceedingly effective and accurate algorithm for impulse noise detection is proposed. Extensive simulation results show that our algorithm has extraordinary ability in identifying impulse noise—achieving zero miss detection rate while keeping false detection rate at a rather low level. Since the detection results will be used to supervise the conduction of filtering that is the most crucial stage under the switching median filtering framework, our algorithm is proven to be more superior than the state-of-the-art algorithms. In the future, we will consider combining various adaptive and iterative filtering mechanisms into current system.

REFERENCES

[1] D. R. K. Brownrigg, "The weighted median filter," *Commun. Assoc. Comput.*, pp. 807–818, Mar. 1984.
[2] S.-J. Ko and Y.-H. Lee, "Center weighted median filters and their applications to image enhancement," *IEEE Trans. Circuits Syst.*, vol. 38, pp. 341–347, Sep. 1991.
[3] T. Sun and Y. Neuvo, "Detail-preserving median based filters in image processing," *Pattern Recognit. Lett.*, vol. 15, no. 4, pp. 341–347, Apr. 1994.
[4] I. Pitas and A. N. Venetsanopoulos, "Order statistics in digital image processing," *Proc. IEEE*, vol. 80, no. 12, pp. 1893–1921, Dec. 1992.
[5] S. Q. Zhang and M. A. Karim, "A new impulse detector for switching median filters," *IEEE Signal Process. Lett.*, vol. 9, no. 11, pp. 360–363, Nov. 2002.
[6] P.-E. Ng and K.-K. Ma, "A switching median fitler with boundary discriminative noise detection for extremely corrupted images," *IEEE Trans. Image Process.*, vol. 15, no. 6, pp. 1506–1516, Jun. 2006.
[7] P. Civicioglu, "Using uncorrupted neighborhoods of the pixels for impulsive noise suppression with ANFIS," *IEEE Trans. Image Process.*, vol. 16, no. 3, pp. 759–773, Mar. 2007.
[8] R. H. Chan, C.-W. Ho, and M. Nikolova, "Salt-and-pepper noise removal by median-type noise detectors and detail-preserving regularization," *IEEE Trans. Image Process.*, vol. 14, no. 10, pp. 1479–1485, Oct. 2005.
[9] L. Bar, N. Sochen, and N. Kiryati, "Image deblurring in the presence of impulsive noise," *Int. J. Comput. Vis.*, vol. 70, no. 3, pp. 279–298, Dec. 2006.
[10] M. Nikolova, "A variational approach to remove outliers and impulse noise," *J. Math. Imag. Vis.*, vol. 20, no. 1–2, pp. 99–120, 2004.
[11] X.-M. Zhang and Y.-L. Xiong, "Impulse noise removal using directional difference based noise detector and adaptive weighted mean filter," *IEEE Signal Process. Lett.*, vol. 16, no. 4, pp. 295–298, Apr. 2009.